

ACOUSTIC NOISE MEASUREMENT METHODOLOGY FOR THE BILLIA CROO WAVE ENERGY TEST SITE ANNEX A: SUMMARY OF OPERATIONAL UNDERWATER NOISE FROM A WAVE ENERGY CONVERTER SYSTEM AT THE EMEC WAVE ENERGY TEST SITE MAY 2011: COMPARASION OF PELAMIS SYSTEM OPERATIONAL AND BASELINE NOISE MEASUREMENTS

Version 1.01 September 2012



ACOUSTIC NOISE MEASUREMENT METHODOLOGY FOR THE BILLIA CROO EUROPEAN MARINE ENERGY CENTRE WAVE ENERGY TEST SITE (EMEC)

ANNEX A: SUMMARY OF OPERATIONAL UNDERWATER NOISE TESTS FOR A PELAMIS P2 SYSTEM AT EMEC MAY 2011

Authors:

Paul Lepper¹, Edward Harland², Stephen Robinson³, Pete Theobald³, Gordon Hastie⁴ & Nichola Quick⁴

- 1) Loughborough University (LU),
- 2) Chickerell BioAcoustics (CBA),
- 3) National Physical Laboratory (NPL),
- 4) Sea Mammal Research Unit Ltd. (SMRU Ltd)

Prepared for:

Jennifer Norris / David Cowan
European Marine Energy Centre (EMEC) Ltd,
Old Academy,
Back Road,
Stromness,
Orkney,
KW16 3AW

Preferred citation:

EMEC report "Acoustic Noise Measurement Methodology for the Billia Croo Wave Energy Test Site: ANNEX A: Summary of operational underwater noise TESTs for a Pelamis P2 system at EMEC May 2011" (Lepper,P., Robinson,S., Harland,E., Theobald,P., Hastie,G., Quick,N. 2012).



EMEC would like to thank the Scottish Government for continued support and funding of this project.

TABLE OF CONTENTS

1	INTRODUCTION	3
2	MEASUREMENT METHODOLOGY	4
2.1	EQUIPMENT SPECIFICATIONS, DEPLOYMENT AND DATA COLLECTION	4
3	RESULTS	9
3.1	MEASUREMENT SUMMARY	9
3.2	TEMPORAL VARIATION (LONG TERM RECORDER ANALYSIS)	10
3.4	SPATIAL VARIATION	15
	<i>Range dependence</i>	15
	<i>Azimuthal variation</i>	17
3.5	EVENT ANALYSIS.....	19
	<i>Clanking</i>	20
	<i>Rattle</i>	22
	<i>Squeak</i>	23
	<i>Sequence of bangs</i>	24
3.6	DRIFTING DEPLOYMENTS.....	25
3.7	COMPARISON PELAMIS SYSTEM AND BASELINE DATA.....	26
3.8	SOURCE LEVEL ESTIMATES	27
3.9	CTD MEASUREMENTS	29
3.10	WEATHER DATA	30
4	SUMMARY	34
5	REFERENCES	36
	ACKNOWLEDGMENTS	37

1 INTRODUCTION

An operational noise assessment was conducted on the Pelamis P2 system at the EMEC wave site in May 2011 by a consortium of Loughborough University, Chickerell BioAcoustics, the National Physical Laboratory and SMRU Ltd. The work is part of a contract from the European Marine Energy Centre (EMEC), Orkney, Scotland to develop an underwater noise measurement methodology for use at the EMEC wave energy test centre. As such the consortium above had developed a provisional measurement methodology based on data from a baseline noise survey (July 2010) [EMEC, 2011a] and review of related materials including previous acoustic work conducted on wave energy systems, likely biological receptors and measurement standards from other industries [EMEC, 2011b]. Trials were then conducted on a Pelamis P2 system in May 2011 with the aim of validating the proposed methodology, these data being used to update and revise the methodology based on lessons learnt [EMEC, 2011c].

In conducting the validation trials a detailed acoustic survey of the Pelamis P2 system was carried out. The aim of this document is to provide a summary of data collected and analyses carried out. Data collected includes long term acoustic data from autonomous recorder units placed on the seabed, wideband boat based drift deployments, CTD casts and analysis of device positional data, weather and oceanographical data.

2 MEASUREMENT METHODOLOGY

2.1 EQUIPMENT SPECIFICATIONS, DEPLOYMENT AND DATA COLLECTION

Underwater sound data was collected using (i) autonomous recording units and (ii) cabled hydrophones deployed from a vessel. Longer-term data collection was made using acoustic recorders on seabed mounted frames. Each frame consisted of a steel tripod with a cross-strut at the base to hold the frame rigid. A hydrophone was mounted at the centre of the frame using nylon rope secured between the top (apex) and bottom strut of the frame, in such a way that it would be suspended in the water without direct contact with the frame or surrounding apparatus. Watertight autonomous recorders were used with each frame to house the recording equipment and electronics. The height of the frame apex was 1.2 m with the triangular base 1.5m length sides. Figure 2-1 a) shows four frames on deck of deployment vessel the Flamborough Light. Figure 2-1 b) shows the autonomous DAQ system and hydrophone on an individual frame.



Figure 2-1a): Assembled frames housing DAQ pod and hydrophone on board, with anchor and weight ready for deployment.



Figure 2-1b): Autonomous DAQ and hydrophone on board mounted on seabed frame.

Each bespoke recording unit is capable of recording up to two channels with a maximum sample rate of 96 kHz sampling to a 24-bit resolution. Systems include digital recorder unit, battery power supply and a specially designed pre-amplifier circuit with adjustable gain. Data is stored in a lossless 'wav' format. Hydrophones on all autonomous systems were 25 mm omni-directional ball hydrophones (HS 70) from SRD Ltd with nominal sensitivity -199 dB re 1 V/ μ Pa. All units have been calibrated to national and international standards.

In addition to the frame recording units, an autonomous Sub-Surface Buoy (SSB) was also used to gather shorter periods of data in various locations. The SSB consisted of two identical SRD Ltd, HS70 hydrophones (sensitivity at 500 Hz -199 dB re 1 V/ μ Pa), mounted on rope and suspended approximately 3 and 5.5 m from the seabed by a marker buoy and float. Figure 2-2 shows a schematic of the deployment configuration.

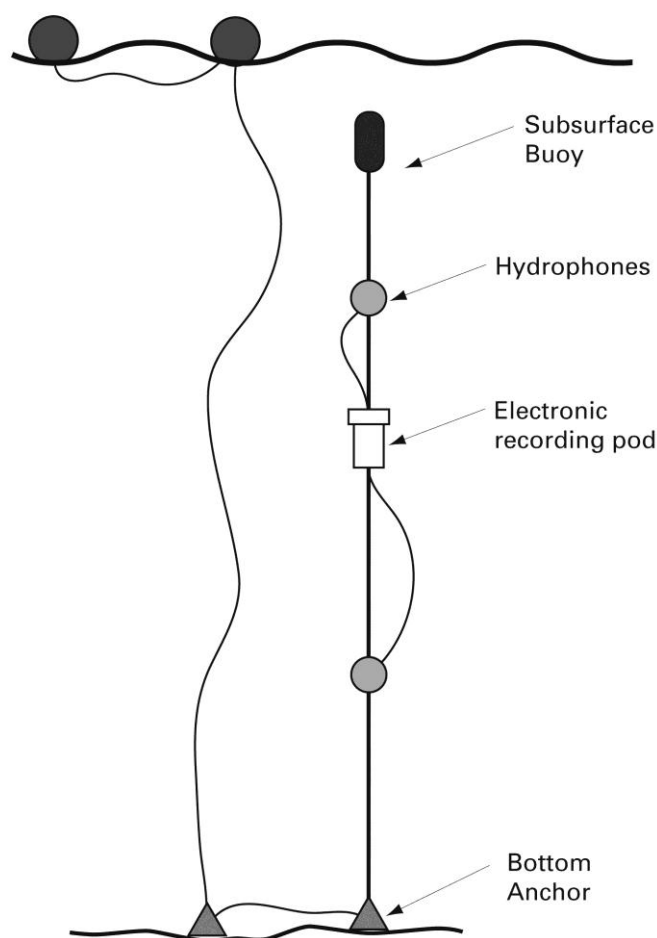


Figure 2-2: Sub-surface buoy (SSB) configuration used for short duration deployments.

Broad band data was recorded from a drifting boat deployment (Figure 2-3). Equipment used included low noise Reson 4032 hydrophones and a broadband Reson 4014 hydrophone. Data acquisition was made using a National Instruments USB DAQ system (NI USB-6251) directly to laptop hard drive using bespoke Labview software. The DAQ system has a maximum aggregate sample rate of 1.25 MS⁻¹ to a 16 bit resolution allowing data acquisition on up to three simultaneous channels to a 150 kHz bandwidth or a 500 kHz

Billia Croo Acoustic Characterisation Final Report – ANNEX A REP375-01-02 20121127
© EMEC 2012

bandwidth on a single channel. All systems were battery powered eliminating the need for generator power during noise measurements minimising both acoustic radiated noise from the vessel and electronic interference. All hydrophones used were calibrated to traceable National and International standards by the National Physical Laboratory across the full frequency band of interest.

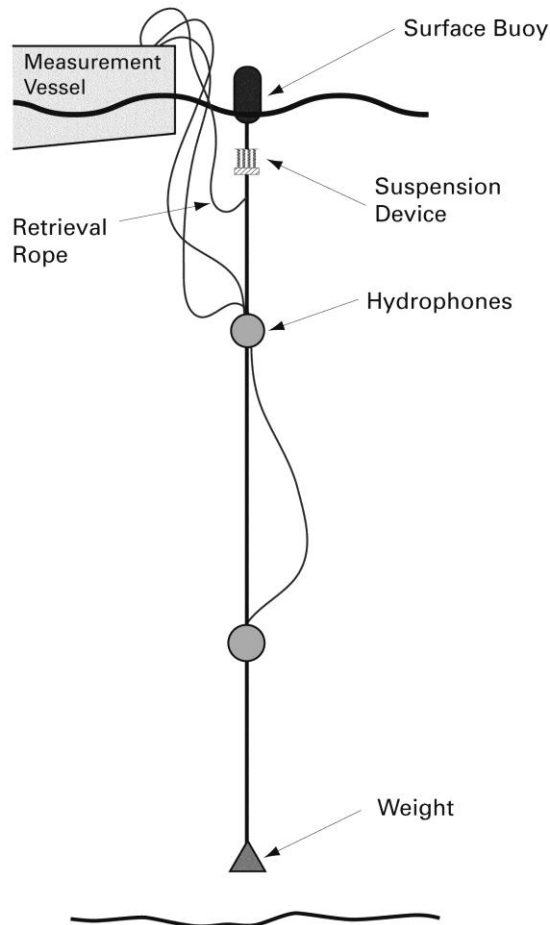


Figure 2-3: Boat-based broadband hydrophone deployments



Figure 2-4: Boat-deployed hydrophones (RESON 4032) ready for deployment.

Deployment and boat-based measurements were made from the local vessel the Flamborough Light. She is a 19 m wooden ex-scalloper based out of Stromness shown in figure 2-5. Vessel and crew are regularly used for deployment work at both EMEC's wave and tidal sites. The Flamborough Light has a large open back deck ideally suited to hydrophone and frame deployment. During boat based work the vessel is allowed to drift 'silent' with all generators / engines off.



Figure 2-5: Deployment vessel the Flamborough Light



Figure 2-6: Pelamis P2 system at the EMEC Billia Croo wave test site

3 RESULTS

3.1 MEASUREMENT SUMMARY

In line with the provisional methodology four seabed mounted autonomous recorder units were deployed on the 11th May 2011 on orthogonal transects on the beam and end-fire positions of the Pelamis system for a period of around 30 hours (figure 3.1). Recorder systems positions have been labelled south outer and south inner on beam aspect transect and north inner and outer on end-fire aspect. Analysis of relative range and position data is discussed in section 3.2 and deployment configuration shown in figure 3-1 & 3-3. A summary of deployment positions is given in table 3-1. Once deployed, systems were left in place allowing analysis of long term trends in acoustic output from the Pelamis system. Four broadband boat based drift trials were conducted in period 11th-12th May 2011 with a maximum measurement range from Pelamis of 2.4 km. Additionally, a sub-surface buoy recorder system was deployed close to Pelamis to operate in parallel with drift deployments. Periodic CTD cast were made on the 10th and 11th May to both the south and north of the Pelamis system.

A summary of all measurement made is provided in table 3-1¹.

Name	Deployment period (UTC + 1)	Location (lat./Lon. WGS84)	Water depth (m)	Description
Outer South	11:17 10 th May - 15:00 11 th May 2011	N58.98191 W3.38761	~50 m	Bottom mounted frame
Inner South	11:21 10 th May - 15:08 11 th May 2011	N58.98243 W3.38850	~50 m	Bottom mounted frame
Inner North	11:28 10 th May - 15:20 11 th May 2011	N58.98545 W3.39000	~50 m	Bottom mounted frame
Outer North	11:33 10 th May 16:26 11 th May 2011	N58.98622 W3.38891		Bottom mounted frame
CTD deployment (1) North	12:04 – 12:09 10 th May 2011	N58.98660 W3.39482 - N58.98662 W3.39487	~50 m	Boat based drifting
CTD deployment (2) South	12:16 – 12:21 10 th May 2011	N58.98141 W3.38561 - N58.98228 W3.38658	~50 m	Boat based drifting
Boat drift measurement (1)	14:18 - 14:47 11 th May 2011	N58.98177 W3.39024 – N58.97959 W3.38516	~50 m	Broadband boat based measurement
CTD deployment (3) North Pelamis	15:35 – 15:40 11 th May 2011	N58.98578 W3.387847 – N58.985667 W3.387642	~50 m	Boat based drifting
CTD deployment (4) North Pelamis	11 th May 2011	N58.982304 W3.387923 – N58.982162 W3.387206	~50 m	Boat based drifting
SSB deployment (1)	10:23 – 12:40 12 th May 2011	N58.98545 W3.39000	~50 m	Sub-surface buoy deployment
Boat drift measurement (2) South cardinal	10:51 – 11:31 12 th May 2011	N58.96223 W3.38803 – N58.96223 W3.38803	~52 m	Broadband boat based measurement
Boat drift measurement (3) East cardinal	10:51 – 11:31 12 th May 2011	N58.97272 W3.36793 – N58.96954 W3.36005	25 - 6 m	Broadband boat based measurement
Boat drift measurement (4) South Pelamis	13:01 – 13:16 12 th May 2011	N58.98204 W3.38974 – N58.98104 W3.38864	~50 m	Broadband boat based measurement

Table 3-1 Measurement summary WEC operational noise trials 10th-12th May 2011

¹ All times reported in this report are based on BST (UTC + 1). GPS positions are in decimalized degrees using WGS84 datum

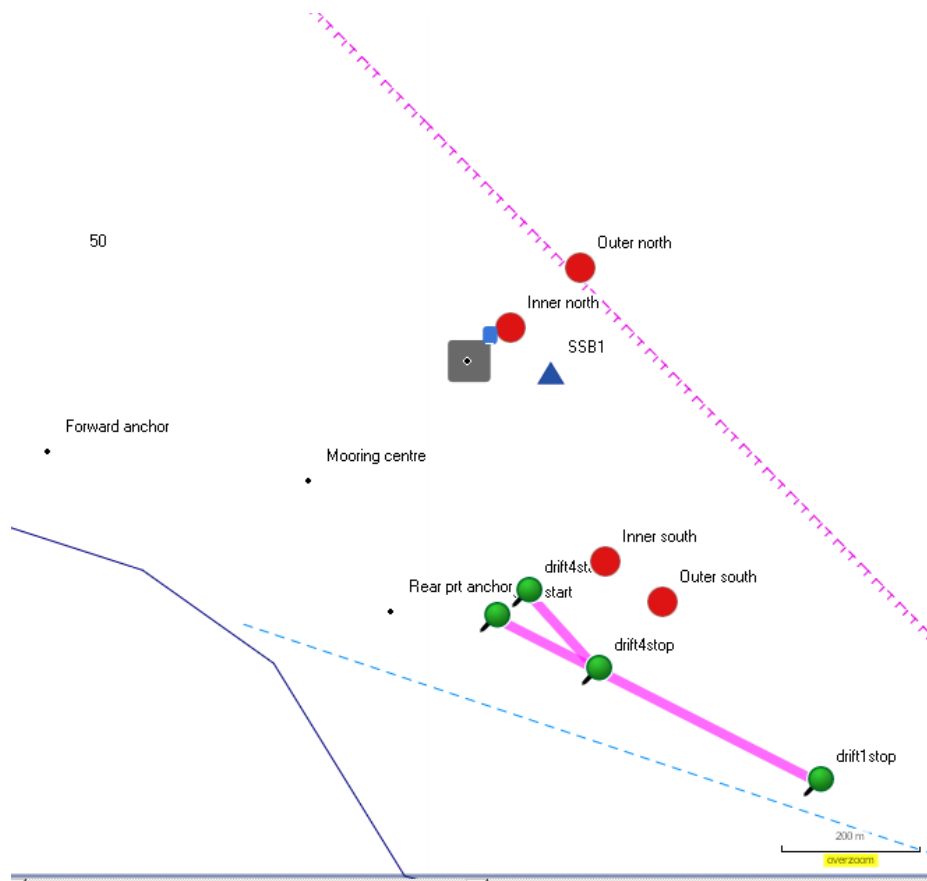


Figure 3-1: Measurements sites Billia Croo (May 2011). (Red circles: recorder deployments; blue: triangle sub-surface buoy deployment; green pins: two closest boat-based drift deployments).

3.2 TEMPORAL VARIATION (LONG TERM RECORDER ANALYSIS)

Four long term recorder systems were deployed on site between 11:17 and 11:33 on the 10th May 2011, systems were nominally positioned in line with provisional measurement methodology proposed with two systems on a beam aspect and two on an end for position. During set up periods the Pelamis system was holding a relatively stable heading of around 225° close to its most northerly motion limit. Figure 3-2 shows averaged (30 minute) heading data from 12:30 on the 10th May 2011 for the entire measurement period. For the first 20 hours of the recorder system deployments the Pelamis stayed within 15° of an average of around between 225° and 240°. Occasional higher variations between 230° and 265° can be seen with a gradual more westerly trend over a 48 hour period up to 270°.

Figure 3-3 shows a schematic of the experimental setup. For a majority of the initial measurement period the two northerly positions were reasonable close to the Pelamis end-fire position (in line with the systems heading). Similarly the two southern systems were placed approximately on the beam aspect but outside the overall system watch circle. With gradual westerly swing of the Pelamis system over 24 hours the heading moved to a position between the two sets of systems.

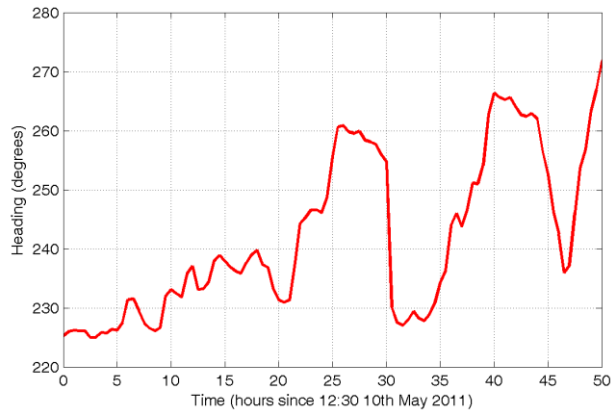


Figure 3-2: Average heading data for Pelamis system from 12:30 10th May 2011. [Data courtesy of Pelamis Wave Power Ltd].

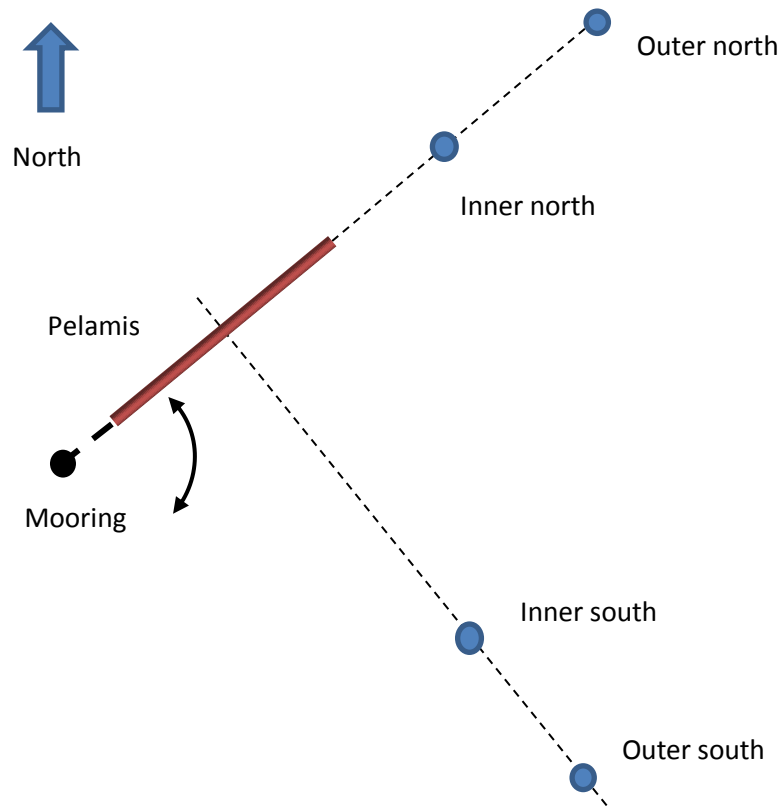


Figure 3-3: Recorder configuration for long term recorder systems 10th-11th May 2011

Figure 3-4 shows 30 minute averaged range from the nose of Pelamis to each recorder station (solid lines). Using heading data shown in figure 3-2 the range to an approximate mid-point along the length of Pelamis system was calculated. The mid-point was chosen as

an arbitrary reference point for later analysis. In this case a point midway between modules 2 and 3 was estimated approximately 84.5 m from the nose position data provided.

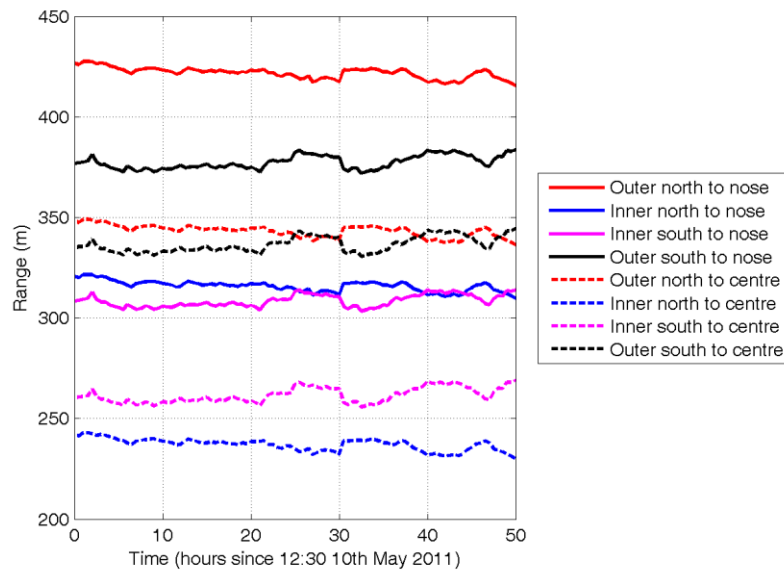


Figure 3-4: Horizontal range to nose and approximate mid-point of Pelamis system from recorder positions.

Figure 3-4 shows that the relative distance of the recorders to both the nose and mid-point positions were relatively stable within the first 24 hours of the deployment. With the two inner systems at horizontal ranges of around 260 m for the southerly and 245 m the northern recorder. Similarly the outer northern recorder was at a range of 345 m and outer southerly recorder around 340 m from the device mid-point. These range estimates can then be directly compared with received levels at each recorder station. It should be noted however that ranges expressed are to an arbitrary reference point approximately mid-way along the device, actual positions of noise source are unknown in current analysis and are likely to be distributed throughout the system. For example, in the end-fire position the inner northern recorder could actually be within 160 m of the end of the Pelamis system.

Figure 3-5 shows an example of long term spectral averaged data for a three hour sequence recorded at the inner southern station around starting at 15:29 on the 10th May. Sequence shows a wide variety of acoustic characteristics with higher temporal and spectral variation. The highest energy contributions are consistently below 2 kHz however occasional higher levels are seen with frequency components greater than 30 kHz. Throughout any one file a number of distinct acoustic events can be identified most likely associated with Pelamis system these are generally below 2 kHz and are intermittent but relatively consistent through all data sequences recorded. These events will be analysed in detail in section 3.5.

The identification of some external noise sources can be made, for example, a significant contribution to the low frequency noise observed gradually reducing within the first 30 minutes of sequence shown in figure 3-5 can be associated with additional boat noise in the area. Similarly a brief increase in noise levels at 18:00 can again be identified as external boat noise. The source of other events such as broadband noise at around 0.85 hours into the sequence with frequency components up to 10 kHz and an increase in broadband noise centred around 15 kHz at approximately 1.8 hours into sequence are not known and may

possible be attributed to the Pelamis operation. Data of the operation status of the Pelamis system (generator on, generator off in individual modules) has been supplied by the Pelamis team post analysis of any correlation may therefore be possible with specific acoustic events.

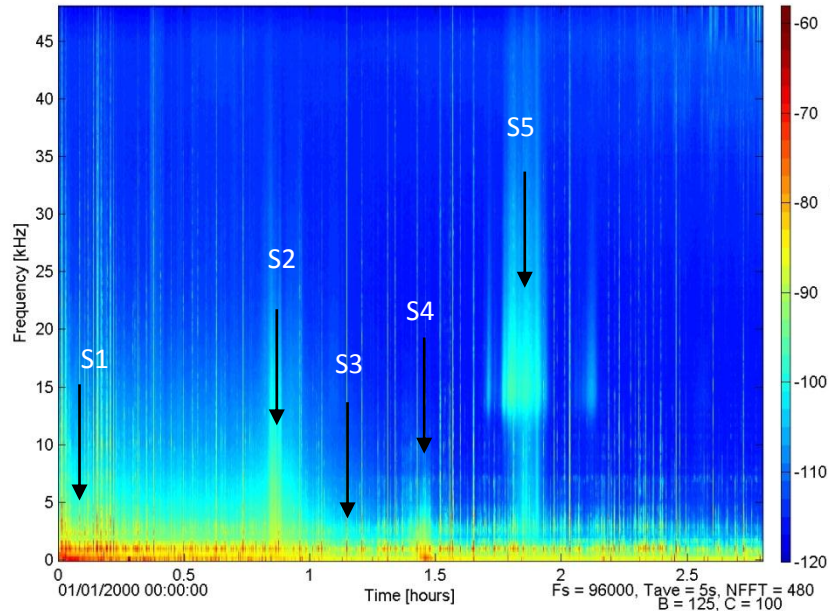


Figure 3-5: Long Term Spectral Average (LTSA) for a three hour period recorded at Inner Southern recorder from 15:29 on 10th May 2011.

The LTSA was generated using the Triton software developed by the Marine Physical Laboratory at UCSD, San Diego. A 5 second average was used with a 480 point linear Fast Fourier Transform (FFT) giving a 200 Hz frequency resolution, with no overlap. Relative amplitude levels are shown on the z-axis colour bar are dB relative to counts²/Hz, where counts are the numeric resolution of the data acquisition system used. For example for a 16 bit system the full dynamic range of the analogue to digital converters used in volts corresponds to a range of $\pm 32,768$ (2^{15}) counts .

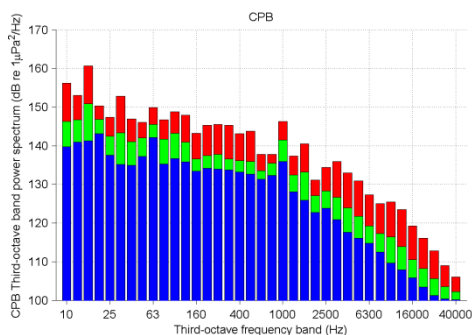


Figure 3-6a: Sequence 1 (S1). 10 minute averaged (15:29-15:39 10th May 2011) Inner South recorder Constant Percentage Bandwidth (CPB) in TOB.

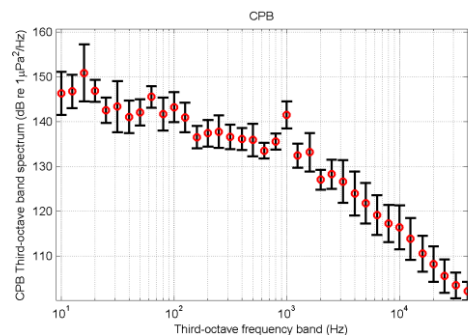


Figure 3-6b: Sequence 1 (S1). 10 minute averaged data (15:29-15:39 10th May 2011) Inner South recorder Constant Percentage Bandwidth (CPB)

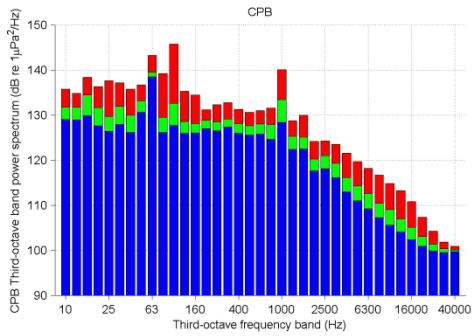


Figure 3-6c: Sequence 2 (S2). 10 minute averaged (16:23-16:33 10th May 2011) Inner South recorder Constant Percentage Bandwidth (CPB) in TOB.

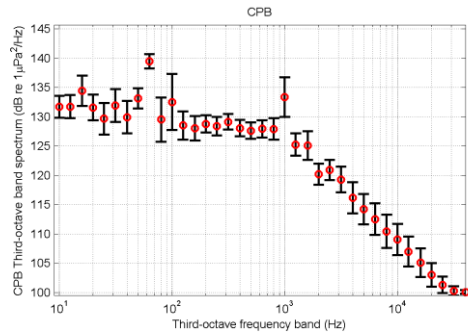


Figure 3-6d: Sequence 2 (S2). 10 minute averaged data (16:23-16:33 10th May 2011) Inner South recorder Constant Percentage Bandwidth (CPB)

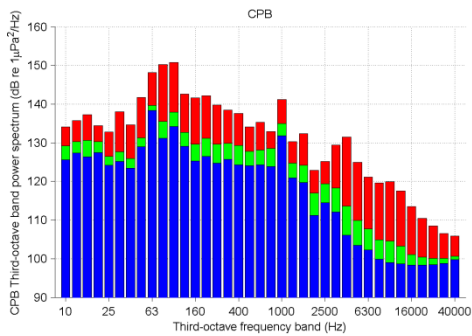


Figure 3-6e: Sequence 3 (S3). 10 minute averaged (16:49-16:59 10th May 2011) Inner South recorder Constant Percentage Bandwidth (CPB) in TOB.

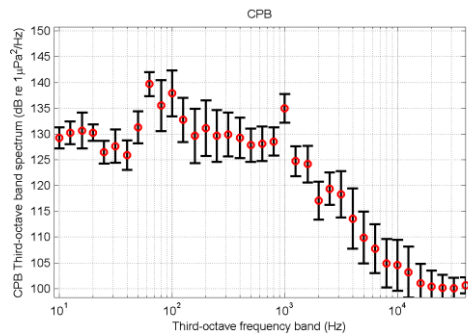


Figure 3-6f: Sequence 3 (S3). 10 minute averaged data (16:49-16:59 10th May 2011) Inner South recorder Constant Percentage Bandwidth (CPB)

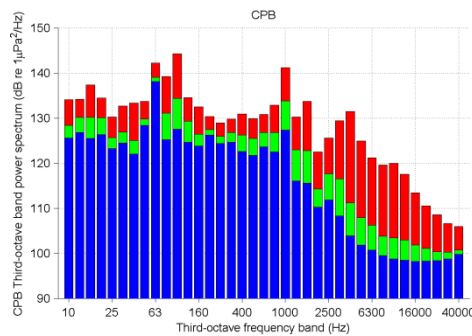


Figure 3-6g: Sequence (S4). 10 minute averaged (17:05-17:15 10th May 2011) Inner South recorder Constant Percentage Bandwidth (CPB) in TOB.

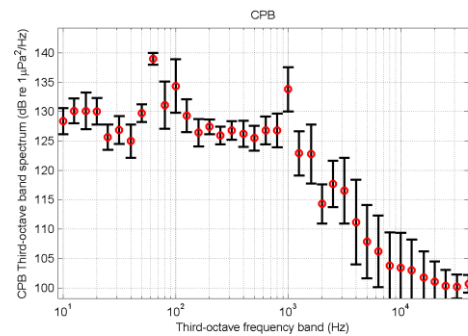


Figure 3-6h: Sequence (S4). 10 minute averaged data (17:05-17:15 10th May 2011) Inner South recorder Constant Percentage Bandwidth (CPB)

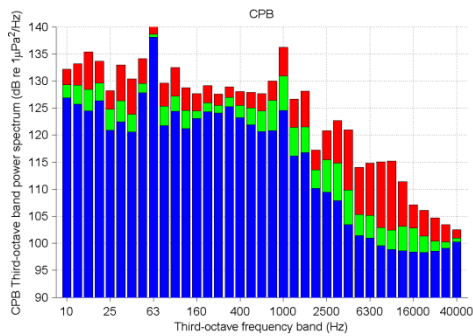


Figure 3-6i: Sequence 5 (S5). 10 minute averaged (17:20-17:30 10th May 2011) Inner South recorder Constant Percentage Bandwidth (CPB) in TOB.

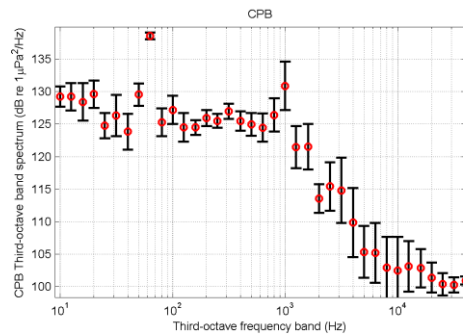


Figure 3-6j: Sequence 5 (S5). 10 minute averaged data (17:20-17:30 10th May 2011) Inner South recorder Constant Percentage Bandwidth (CPB)

Figure 3-6 a-i: Constant percentage bandwidth (CPB) power in third octave bands. 10 minute averaged. Left side maximum (red), mean (green) and minimum (blue) data integrated over consecutive a 40 s period across entire 10 minute sequence. Right side power across third octave bands integrated across consecutive across 1 s windows. Red circles mean values, bars ± 1 standard deviation. All analysis is received level at the recorder.

Figure 3-6 (a-i) shows averaged received level data integrated across consecutive 40 second blocks over a 10 minute period for the inner southern recorder. Sequence S1 (figures 3-6a and 3-6b) and S4 (figures 3-6g and 3-6h) show relatively high low frequency components present, potentially associated with boat noise in the vicinity. Comparison with data when no boat is present can be seen in the third sequence S3 (figure 3-6e and 3-6f). This shows levels at frequencies below 63 Hz (roughly 15-20 dB lower). All the plots show relatively consistent components in the 1 kHz third octave band. In sequence 1 this is around 140 dB re 1 $\mu\text{Pa}^2/\text{Hz}$ dropping to values between 130 and 135 dB for the later sequences. These components in band 500 Hz- 2 kHz can be seen in long term spectral averaged data consistently throughout the entire recording. Figures 3-6i and 3-6j show slightly elevated levels at higher frequencies, around 16 kHz, rising to a received level of around 104 dB re 1 $\mu\text{Pa}^2/\text{Hz}$. this is consistent with data seen in figure 3-6. It should be noted that data in 4-6 shows received level with an approximated horizontal range for device mid-point of around 260 m and 305 m from the nose of the device.

3.3 SPATIAL VARIATION

Range dependence

Overall received levels at some distance from the device are dependent on the ‘loudness’ at the source and propagation losses. In the latter case losses are dependent on the environment including parameter such as water depth, seabed bathymetry sound speed profile, sediment type etc. In relatively shallow waters these parameters can result in significant variation in received levels with range.

Figures 3-7, 3-8 & 3-9 show received level data for a 10 minute averaged sequence starting at 16:29 10th May 2011. The sequence is in a relatively quiet period with no additional boat noise observed in data (between sequences S2 and S3 figure 3-5). At this time it is assumed that the major contributions to the noise field are due to the presence of the Pelamis system. Data presented is recorded simultaneously from the two southern recorder positions in this case the systems were relatively close to an orthogonal transect to the

beam aspect of the device approximately in line with device midpoint (figure 3-3). The inner recorder (a) is shown on left and correspond outer recorder data on right (b). Estimated horizontal ranges to recorders from device midpoint were 256 m and 333 m for inner and outer recorders respectively (figure 3-4).

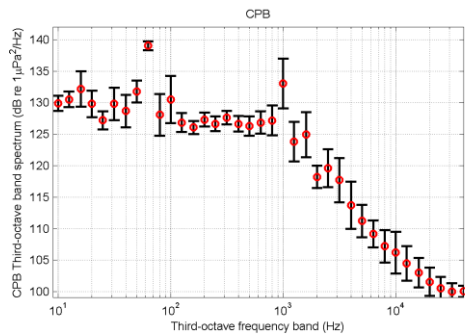


Figure 3-7a: 10 minute averaged Third octave band CPB received Levels at the Southern Inner recorder system. Beam aspect: Approximate horizontal range to device midpoint 256 m

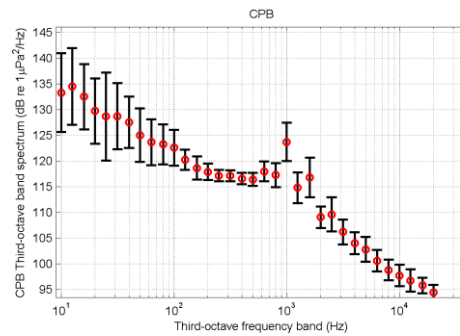


Figure 3-7b: 10 minute averaged Third octave band CPB received Levels at the Southern Outer recorder system. Beam aspect: Approximate horizontal range to device midpoint 333 m

(Red circles mean values, bars \pm 1 standard deviation. All analysis is received level at the recorder, approximate horizontal range to device mid-point around) Data interrelated across 40 second intervals averaged over a 10 minute sequence.

For frequencies from around 100 Hz – 1 kHz the third octave band spectral energies are generally approximately 10 dB lower on outer recorder system consistent with potential propagation losses with increased range. A strong 1 kHz band energy component can be seen in both recordings with mean levels of 133 dB re 1 $\mu\text{Pa}^2/\text{Hz}$ at the closer recorder dropping to 128 dB re 1 $\mu\text{Pa}^2/\text{Hz}$ at the outer recorder system. Similar difference between systems of around 2- 5 dB can be seen for frequencies greater than 1 kHz. However the outer system shows occasional slightly higher levels at lower frequencies (<50 Hz) suggesting energy coming from other sources. The inner system also shows a strong energy component in the 63 Hz band not observed in the outer recorder systems.

Figures 3-8 shows the equivalent data with averaged maximum and minimum levels and figure 3-9 the equivalent absolute received levels during the 10 minute sequence. Note slightly higher variation in the lower frequencies for the outer recorder resulting higher standard deviations seen in figure 3-7b.

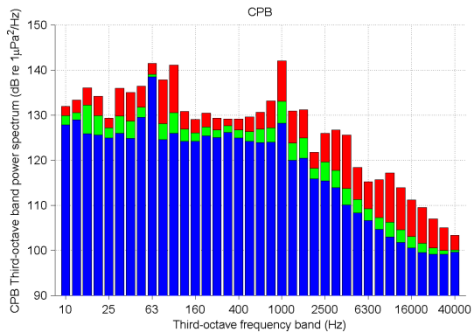


Figure 3-8a: 10 minute averaged CPB received level in third octave bands. Southern Inner recorder system. Beam aspect: Approximate horizontal range to device midpoint 256 m

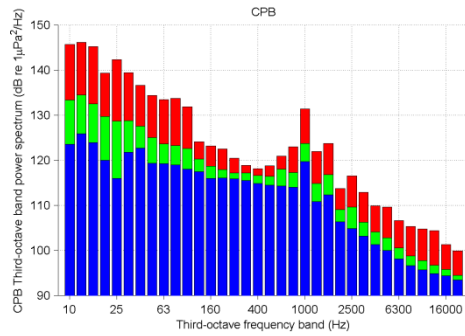


Figure 3-8b: 10 minute averaged CPB received level in third octave bands. Southern Outer recorder system. Beam aspect: Approximate horizontal range to device midpoint 333 m

Maximum (red), mean (green) and minimum (blue) data integrated over consecutive a 40 s period across entire 10 minute sequence.

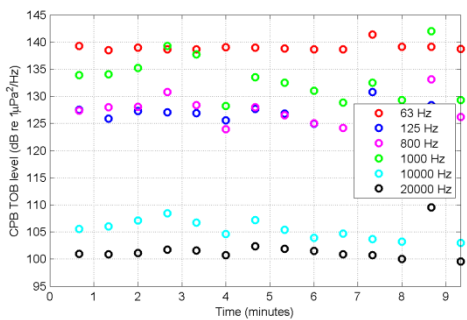


Figure 3-9a: Selected TOB received level in third octave bands. Southern Inner recorder system. Beam aspect: Approximate horizontal range to device midpoint 256 m

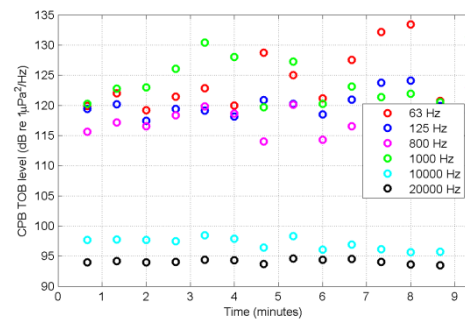


Figure 3-9b: Selected TOB received level in third octave bands. Southern Outer recorder system. Beam aspect: Approximate horizontal range to device midpoint 333 m

Data integrated over consecutive a 40 s period across entire 10 minute sequence.

Azimuthal variation

Comparison of azimuthal variations is particularly problematic in the case of an extended distributed source such as the Pelamis. From figure 3-3 it can be seen that in the end-fire positions the two northern recorders may receive energy from anywhere along the system. With potential range variation compared to the device midpoint positions of around ± 87 m (approximately the half length of the Pelamis system). At shorter ranges this variation can make significant differences in propagation loss between the system and the recorders. Figure 3-10 shows the simultaneous data from two beam aspect positions (southern inner and outer) and the further end-fire position (northern outer). Data from the inner northern site was not used in this analysis due to noise contamination.

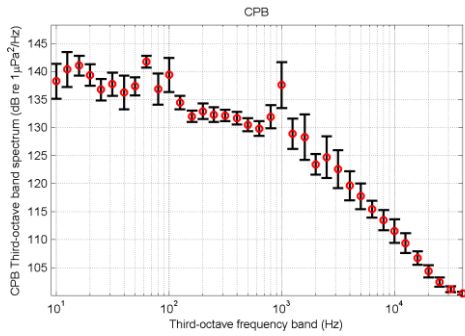


Figure 3-10a: 10 minute averaged CPB received level in third octave bands.

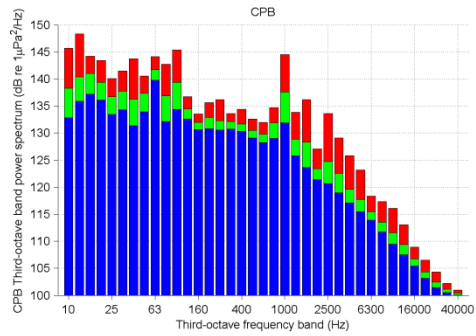


Figure 3-10b: 10 minute averaged CPB received level in third octave bands.

Inner South (beam aspect: range to device midpoint ~256 m)

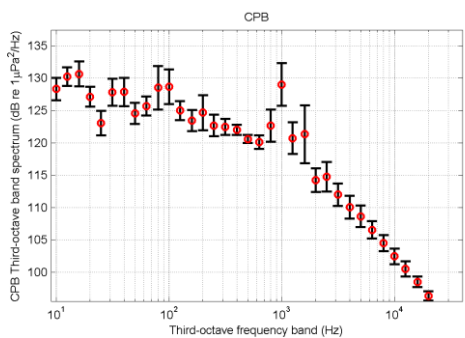


Figure 3-10c: 10 minute averaged CPB received level in third octave bands.

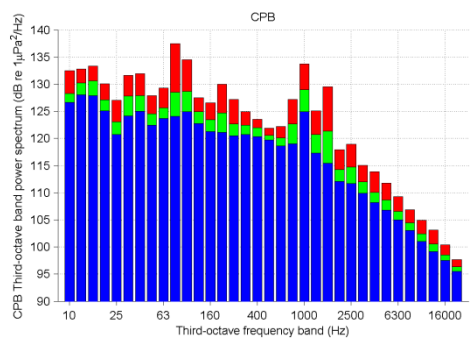


Figure 3-10d: 10 minute averaged CPB received level in third octave bands.

Outer South (beam aspect: range to device midpoint ~333 m)

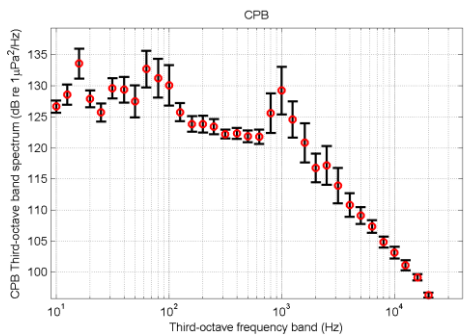


Figure 3-10e: 10 minute averaged CPB received level in third octave bands.

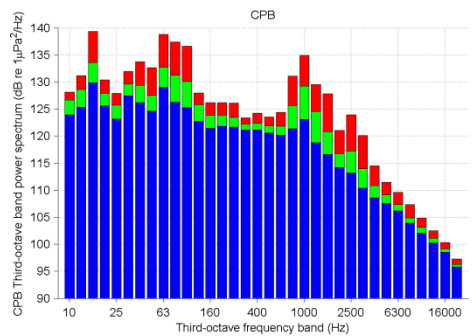


Figure 3-10f: 10 minute averaged CPB received level in third octave bands.

Outer North (end-fire: range to device midpoint ~345 m)

Left: (Red circles mean values, bars ± 1 standard deviation. All analysis is received level at the recorder, approximate horizontal range to device mid-point around) Data interrelated across 40 second intervals averaged over a 10 minute sequence. Right Maximum (red), mean (green) and minimum (blue) data integrated over consecutive a 40 s period across entire 10 minute sequence.

Data from all three position show with a number of features again with strong energy

components in the TOB around 1 kHz and increased levels in bands between 60 and 200 Hz. The highest mean levels in the 1 kHz band can be seen at the southern inner station (beam aspect) of around 137 dB re 1 $\mu\text{Pa}^2/\text{Hz}$ compared with mean values 8 dB lower of around 129 dB re 1 $\mu\text{Pa}^2/\text{Hz}$ at the two outer stations. Similarly for frequency bands below 1 kHz levels are generally 5-6 dB higher at the closer inner southern station with similar levels seen at the two outer stations. Generally levels are similar for the two outer stations on both end fire and beam aspect. Note both outer stations are at similar ranges from chosen reference point midway along the device. The outer end fire position does however show higher levels in the low frequency band centred on 16 Hz not seen in the southern outer recorder but seen on the closer southern system.

3.4 EVENT ANALYSIS

Detailed analysis of acoustic data shows a number of short term acoustic events most likely associated with the Pelamis system. These are likely directly related to specific mechanical, electrical / hydraulic operations within the system. The most dominant events are analysed in detail below, although the exact sources are unknown descriptive names have been assigned to illustrative purposes. Further analysis with Pelamis engineers is likely to be able to assign specific systems operation to acoustic outputs. These events occur intermittently and with no apparent correlation although most likely linked to specific device components / operations. All events may be contributing to overall noise levels seen in short term averaged data analysed in section 3.4 depending on regularity of occurrence and levels.

Data shown in the following analysis is from the Southernmost recorder around 16:05 on the 10th May 2011. Figure 3-11 shows a sample period in which a number of noise events occur.

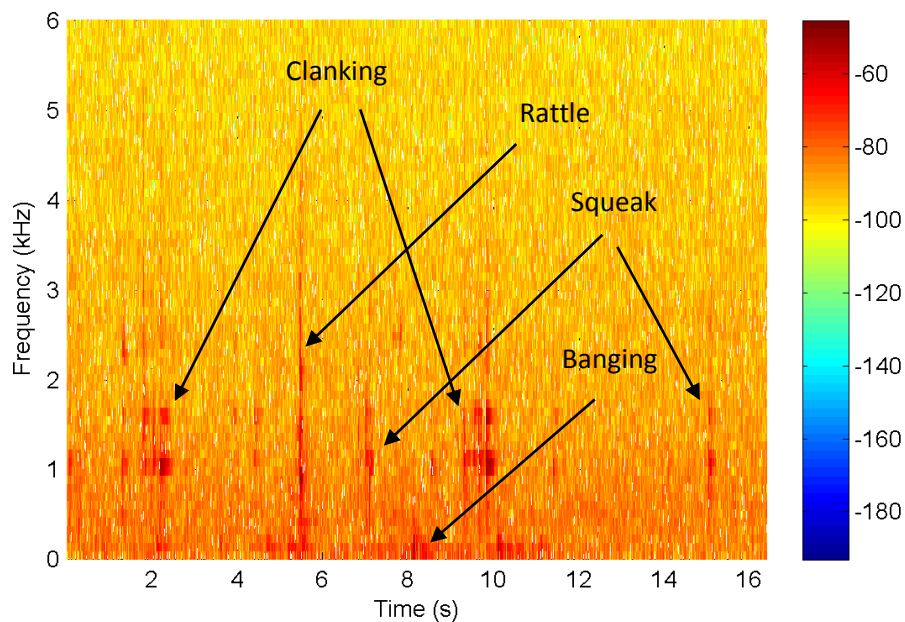


Figure 3-11: Time versus frequency spectrogram of example short term noise events. Southern most recorder station 16:10 10th May 2011. Range from recorder to device midpoint 333m.

Clanking

Much of the low frequency noise is dominated by regular ‘clanking’ noise consistent with noise from chains. Figure 3-12 a-c show a relatively stable frequency component with components in the 1 kHz band and secondary component at 1.5 kHz.

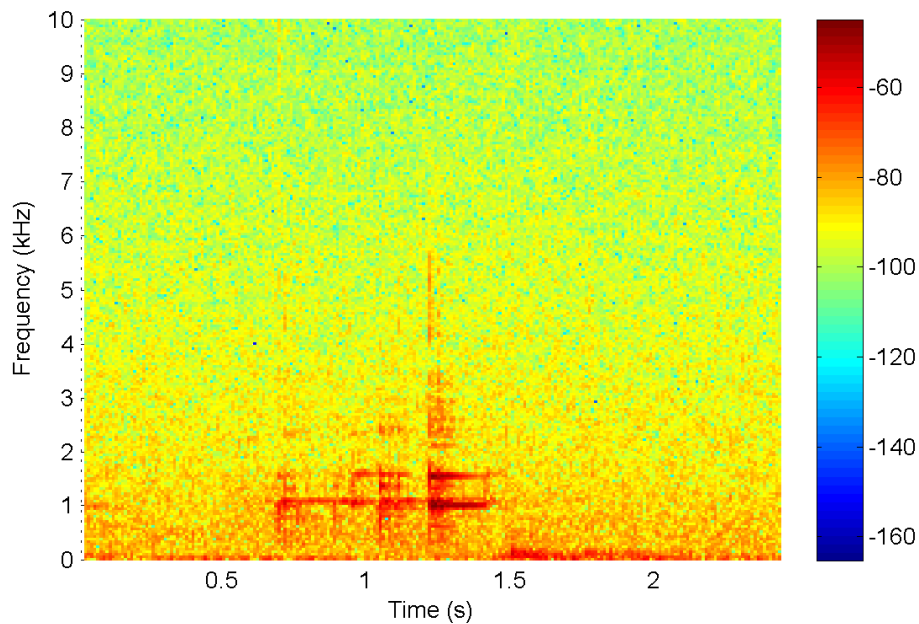


Figure 3-12a: Normalized spectral level for ‘clanking’ noise Southern most recorder station 16:10 10th May 2011. Range from recorder to device midpoint 333m.

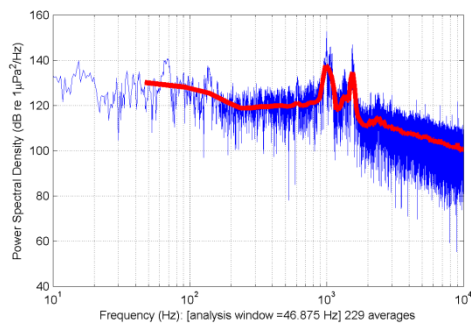


Figure 3-12b: ‘clanking’ noise linear and Welch averaged power spectral density across entire period of spectrogram shown above

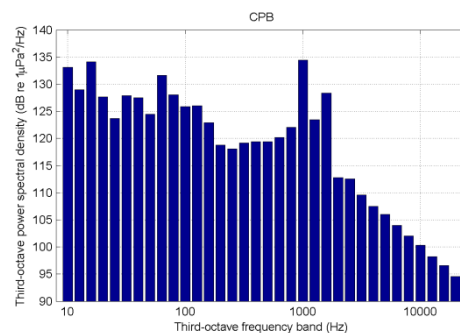


Figure 3-12c: ‘clanking’ noise Constant percentage bandwidth Power spectral Density in third octave bands integrated across entire time window shown in spectrogram above

Analysis shows high level components at approximately both 1.0 and 1.5 kHz with additional frequency components extending up to greater than 5 kHz. Received Levels are

around 135 dB re 1 $\mu\text{Pa}^2/\text{Hz}$ in third octave bands and 139 dB re 1 $\mu\text{Pa}^2/\text{Hz}$ power spectral levels at 1 kHz with a secondary 1.5 kHz component around 5-6 dB lower.

Rattle

Another component that is observed less frequently is described as a rattle. Figure 3-13 a-c shows a strong component around 2.5 kHz and a lower level components between 5 and 6.6 kHz. The primary levels are around 117 dB re $1 \mu\text{Pa}^2/\text{Hz}$ in third octave band and 120 dB re $1 \mu\text{Pa}^2/\text{Hz}$ power spectral levels using Welch averaged data across the sequence shown in figure 4-13. The 1 kHz components seen in TOB analysis and the power spectral density analysis most likely due to examples of clanking noise as that seen in figure 4-12. Levels are generally around 20 dB lower than those observed from the clanking noise.

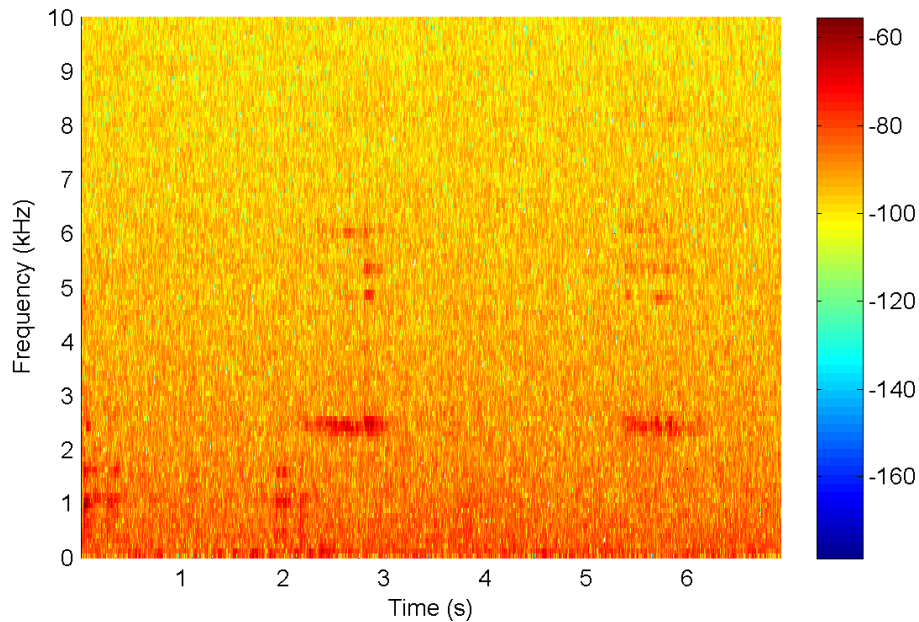


Figure 3-13a: Normalized spectral level for 'rattle' noise. Southern most recorder station 16:10 10th May 2011. Range from recorder to device midpoint 333m.

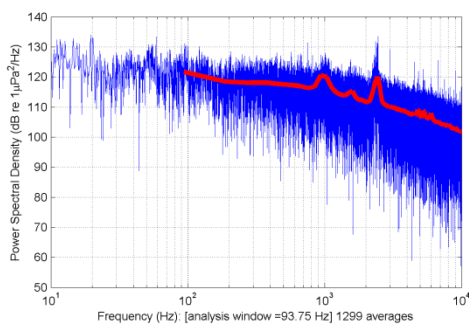


Figure 3-13b: 'rattle' noise FFT and Welch averaged power spectral density across entire period of spectrogram shown above

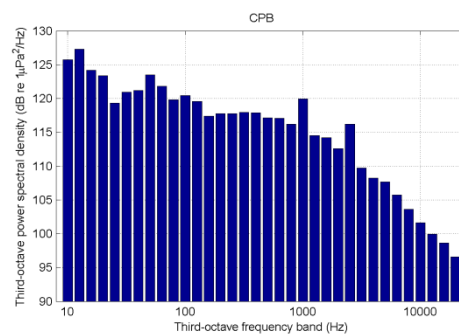


Figure 3-13c: 'rattle' noise constant percentage bandwidth Power spectral Density in third octave bands integrated across entire time window shown in spectrogram above

Squeak

Another regularly occurring noise can be described as a ‘squeak’ this has a slight up and down sweep in frequency over a narrow band centred on 900 Hz shown in figure 3-14 a-c. Data shows Welch averaged received levels of 127 dB re 1 $\mu\text{Pa}^2/\text{Hz}$ and third octave band and 125 dB re 1 $\mu\text{Pa}^2/\text{Hz}$ in the closest third octave band. The Squeak duration can be in excesses of 0.5 s.

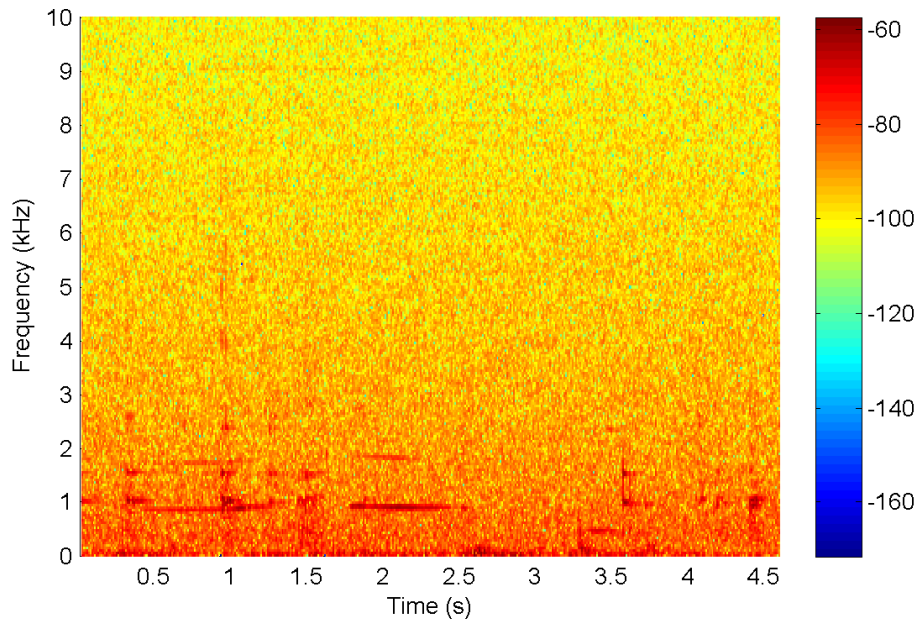


Figure 3-14a: Normalized spectral level for ‘squeak’ noise. Southern most recorder station 16:10 10th May 2011. Range from recorder to device midpoint 333m.

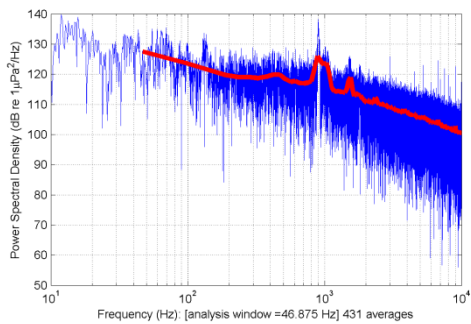


Figure 3-14b: ‘squeak’ noise FFT and Welch averaged power spectral density across entire period of spectrogram shown above

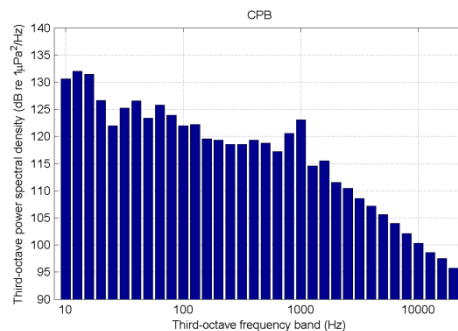


Figure 3-14c: ‘squeak’ noise constant percentage bandwidth Power spectral Density in third octave bands integrated across entire time window shown in spectrogram above

Sequence of bangs

Another less regularly occurring noise can be described as a sequence of ‘bangs’ at relatively low frequencies of around 100 Hz as shown in figure 3-15 a-c. Received levels at the from data show Welch averaged received levels of 150 dB re 1 $\mu\text{Pa}^2/\text{Hz}$ at 100 Hz and 145 dB in the closest third octave band. Sequence duration again in order of 0.5 - 1 s.

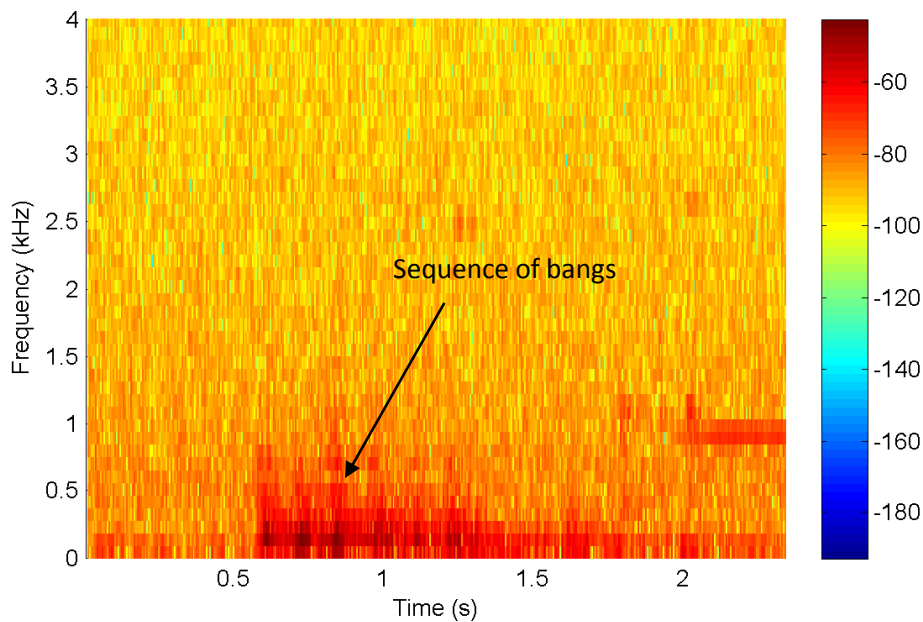


Figure 3-15a: Normalized spectral level for ‘Bangs’ noise. Southern most recorder station 16:10 10th May 2011. Range from recorder to device midpoint 333m.

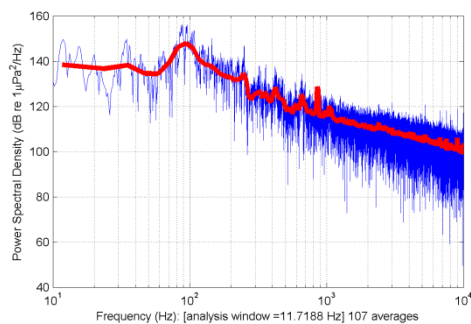


Figure 3-15b: Sequence of ‘bangs’ noise FFT and Welch averaged power spectral density across entire period of spectrogram shown above

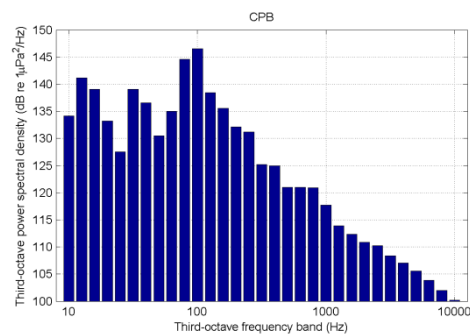


Figure 3-15c: ‘Bangs’ noise constant percentage bandwidth Power spectral Density in third octave bands integrated across entire time window shown in spectrogram above

All of the above noises occur throughout all data sets analysed and appear to contribute significantly to the radiated output of the device seen in the averaged data sets. Additional

continuous broadband noise sources (potentially associated with generators etc.) also appear to be present however direct separation of source from other factors has not been possible in current data sets.

3.5 DRIFTING DEPLOYMENTS

Four drifting deployments were made from the Flamborough Light between the 11-12th May 2011 at the Billia Croo site using broadband recording equipment. These included a south of Pelamis (drift1) on the 11th, and on the 12th close to the south cardinal at a range of around 2.4 km from the device (drift2), in shallow water east of the east cardinal (drift 3) and again just to the south of Pelamis (drift 4). On the 12th weather conditions were significantly better with significant wave heights of average 63 cm and wind speed of 1.3ms⁻¹. Drift deployment positions are shown in figure 4-16.

Two hydrophones were used at a depth of 10 m. A low noise Reson 4032 and a wider bandwidth Reson 4014. Anti-surge mechanisms were used in line with figure 2-3. The Flamborough light was made 'quiet' and allowed to drift with all engines and generators off. All recording equipment was run on battery power. In addition a sub-surface buoy system was also deployed just to north of Pelamis in line with figure 2-2 between 10:30 and 12:40 on the 12th May whilst drift deployments were conducted.

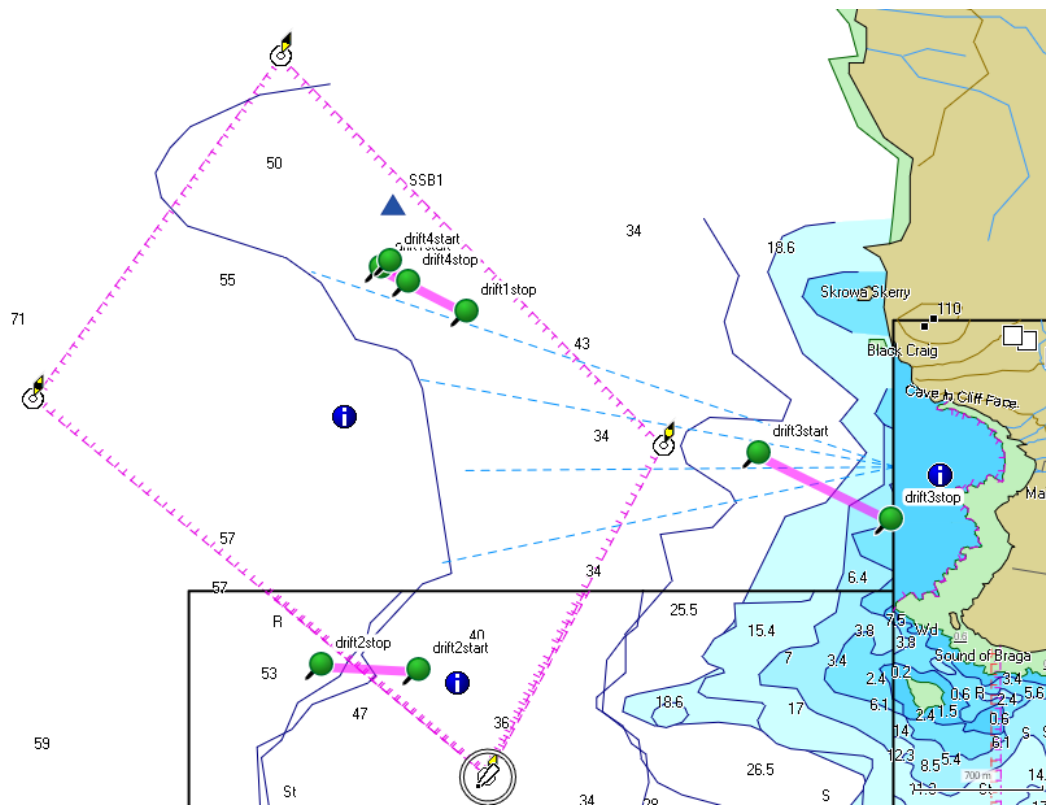


Figure 3-16: Boat based drift deployment 11th and 12th May 2011.

Data was analysed over 10 minute sequences up to a 150 kHz bandwidth to produce averaged data from consecutive 40 second integration periods across the sequence as used with previous analysis. The mean, minimum and maximum third octave band (TOB) power

and the mean constant percentage bandwidth with ± 1 standard deviation of sampled data from the two further drifts are shown in figure 3-17 a-d.

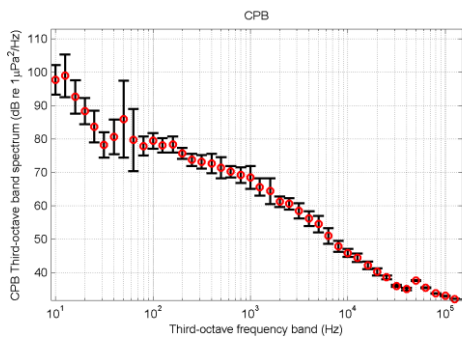


Figure 3-17a: 10 minute averaged CPB received level in third octave bands.

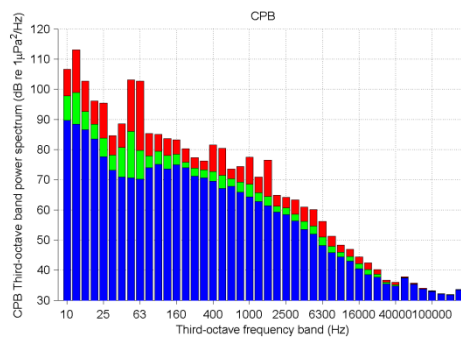


Figure 3-17b: 10 minute averaged CPB received level in third octave bands.

Drift 2 (Near south cardinal 12th May 2011 ~ range to midpoint 2.4 km)

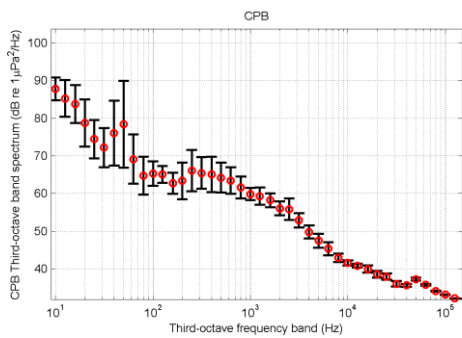


Figure 3-17c: 10 minute averaged CPB received level in third octave bands.

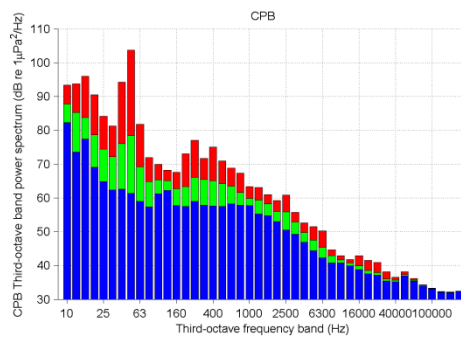


Figure 3-17f: 10 minute averaged CPB received level in third octave bands.

Drift 3 (Near east cardinal 12th May 2011 ~ range to device midpoint 2 km)

Left: (Red circles mean values, bars ± 1 standard deviation. All analysis is received level at the recorder, approximate horizontal range to device mid-point around) Data interrelated across 40 second intervals averaged over a 10 minute sequence. Right Maximum (red), mean (green) and minimum (blue) data integrated over consecutive a 40 s period across entire 10 minute sequence.

Levels are significantly lower than observed at shorter ranges in short term analysis described above for the bottom mounted recorders consistent with increased propagation loss and changes in operational status. Detailed analysis of specific events shows similar features to this described in section 4-5 can still be observed at longer ranges but at lower levels. Note that these drift trials were conducted in good weather conditions (sea state 1-2) resulting on lower background noise levels seen in figure 3-17 and in baseline report (EMEC, 2011a). Under increased ambient noise conditions these feature may no longer be detectable at longer ranges.

3.6 COMPARISON PELAMIS SYSTEM AND BASELINE DATA

Direct comparison of baseline and operational noise data is difficult due to the potentially wide variation of ambient noise levels with and without the Pelamis P2 system on site, as

shown in the baseline survey report [EMEC, 2011b]. Some comparison is however attempted under similar conditions using data from both measurement periods. Figures 3-18 and 3-19 show both baseline and measured received level spectral outputs under similar sea-state conditions. In the case of Figure 3-18 comparison can be made with red circles showing the 10 minute averaged data from the inner southern seabed recorder on 10th May 2011 at an approximate range of 256 m from the Pelamis system midpoint. The blue circle show the equivalent 10 minute averaged data taken from the Northern bottom mounted recorder during the baseline measurement on the 26th July 2010. During baseline trials average significant wave height was around 100 cm with wind speeds 4-5 ms⁻¹. During measurement operational noise trials in May 2011 significant wave heights were 70-80 cm but with slightly higher wind speed of 5-6 ms⁻¹. Through most frequency bands elevated levels with the Pelamis system present in relation to the mean baseline values on site can be seen. The maximum increase in levels with Pelamis system present in the range 10-20 dB. During the baseline study no significant 1 kHz component was observed compared with the Pelamis operational noise measurements.

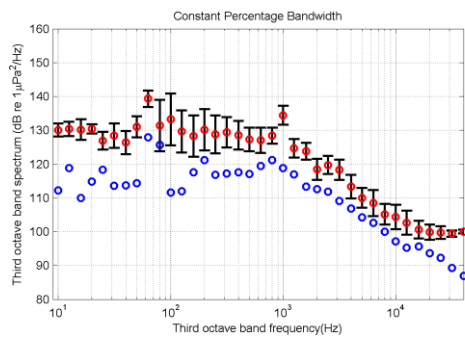


Figure 3-18: Red circles 10 minute mean data from 16:49-16:59 on the 10th May 2011 on the Inner South recorder with Pelamis present, bars \pm 1 standard deviation. Blue circles the northern recorder on 14:12-14:22 on the 26th July 2010 during baseline measurements without Pelamis present. Beaufort scale 3-4.

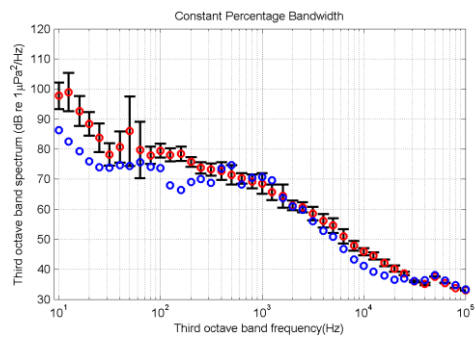


Figure 3-19: Red circles 10 minute mean data from 13:01 – 13:16 on 12th May 2011 on the Inner South recorder with Pelamis present, bars \pm 1 standard deviation. Blue circles the northern recorder on 10:51 – 11:31 12th May 2011 during baseline measurements without Pelamis present. Beaufort scale 1-2.

Figure 3-19 shows comparison of broadband boat based drift measurements made on the 12th May 2011. The red circles and bars show average and standard deviation for a drift measurement between 13:01 – 13:16 on 12th May 2011 at an average range of 238 m from Pelamis midpoint. The blue circles show the average data from 10:51 – 11:31 12th May 2011 at an average range of 2.4 km from Pelamis. Data from the 12th May shown in figure 4-19 represent a lower sea state than that seen in baseline trials and on the 10th of May 2011 (shown in figure 4-18) with significant wave heights around 50-60 cm with lower wind speeds in region 1-2 ms⁻¹ representing a Beaufort scale 1-2. Figure 4-19 shows slightly elevated levels in frequency bands below 500 Hz for the close site compared to the distant measurements. Neither data sets show significant presence of 1 kHz components observed at higher sea states. Maximum increase in level during operational trials of around 10 dB was observed for frequencies below 500 Hz. A slight elevation again can be seen for frequencies 10-20 kHz of maximum value of around 5 dB.

3.7 SOURCE LEVEL ESTIMATES

Using data shown in figures 3-18 and 3-19 approximate 'source level' estimates can be made. Because of the distributed nature of the WEC system, however, ranges from receiver Billia Croo Acoustic Characterisation Final Report – ANNEX A REP375-01-02 20121127
© EMEC 2012

to individual source components is unknown, therefore a composite field measured at some distance away from the system may be comprised source with variable propagation range [EMEC, 2011c]. The assumption of range was therefore made to an arbitrary mid-point along the WEC length. It should be noted that actual distance may be greater and therefore an underestimation of potential source levels from individual noise components.

A Parabolic Equation (RAM [Collins, 1993]) propagation loss models were run for profile from system mid-point to inner southern recorder at a range of 256 m on the beam aspect using the ActUp software suite [Maggi and Duncan, 2010]. The source was assumed to be 1 m from the surface and receiver close to seabed. A uniform coarse sand sediment profile was used in this example and sound velocity taken from data presented in section 3.9. Note data suggests that profiles from area of the WEC system are likely to be a mixture of sediment types ranging from coarse sand, rocks and broken shells. All these sediments are relatively acoustically reflective (higher impedance) than other more lossy sediment types for example silts and muds. The use of a uniform sand profile was felt more precautionary in this simplified example. Each range profile was run for third octave band centre frequencies from 10 Hz – 2 kHz.

Figure 3-20 and 3-21 show examples of the transmission loss profile to a range of 3 km for 125 Hz and 1000 kHz signals respectively. Note more complex but generally higher losses at the higher frequency.

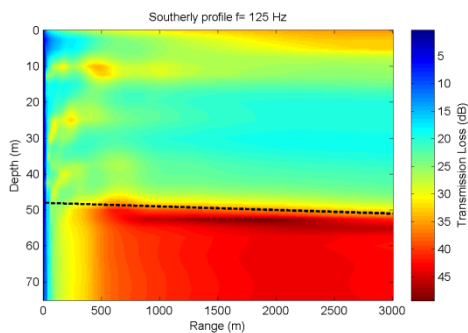


Figure 3-20: 125 Hz transmission loss profile for a beam aspect (southerly) transect. Dashed line represents seabed interface.

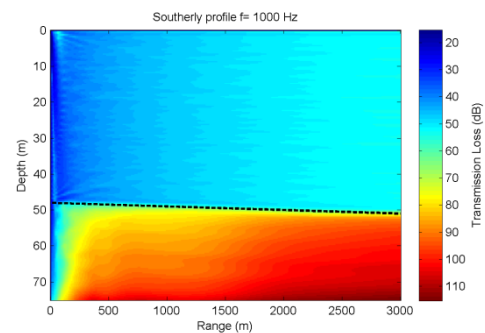


Figure 3-21: 100 Hz transmission loss profile for a beam aspect (southerly) transect. Dashed line represents seabed interface.

Loss profiles in each band were then combined with equivalent received levels recorded at the inner southern recorder, shown in figures 3-18 and 3-19. The equivalent source level to a device midpoint under different sea state conditions is then given in figures 3-22 and 3-23. Figure 3-22 shows an equivalent average source levels of around 181 dB re $1\mu\text{Pa}^2\text{Hz}^{-1}\text{-m}^2$ at around 1 kHz based from data with a sea-state 3-4 with most bands in range 10 Hz – 2 kHz greater than 140 dB re $1\mu\text{Pa}^2\text{Hz}^{-1}\text{-m}^2$. The equivalent 1 kHz band in lower sea state shown in figure 3-22 is around 120 dB re $1\mu\text{Pa}^2\text{Hz}^{-1}\text{-m}^2$. The blue circles in both plots show the baseline received levels during a relatively ‘quite’ sea states (*Beaufort scale 1-2*).

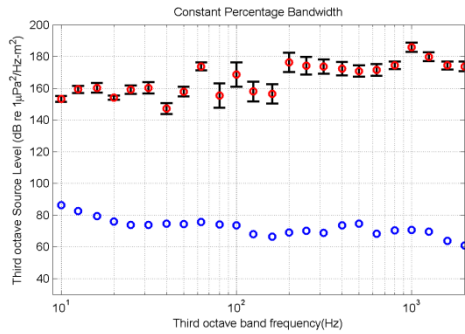


Figure 3-22: Red circles 10 minute mean Source Level estimate data from 16:49-16:59 on the 10th May 2011 on the Inner South recorder with Pelamis present, bars ± 1 standard deviation Beaufort scale 3-4. Blue circles baseline received level measurements without Pelamis present Beaufort scale 1-2.

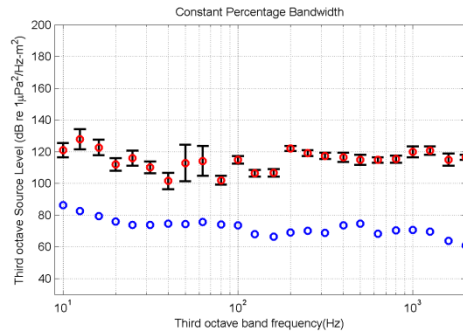


Figure 3-23: Red circles 10 minute mean Source Level data from 13:01 – 13:16 on 12th May 2011 on the Inner South recorder with Pelamis present, bars ± 1 standard deviation. Beaufort scale 1-2. Blue circles the equivalent baseline received level measurements without Pelamis present. Beaufort scale 1-2.

3.8 CTD MEASUREMENTS

Both up and down CTD casts were conducted periodically both at the Billia Croo site, two on the 10th May and two on the 11th. On both days casts were made to the north and south of the Pelamis position. Figure 3-24 shows data from Billia Croo. Both profiles show relatively stable profile for depths below 5 m with a value of around 1488 ms⁻¹. Dropping slightly lower at depths below 30 m. However higher velocity were seen close to the surface in the case of the data from the 11th sound velocity is nearly 5 ms⁻¹ higher in last few meters near surface. This effect could make significant difference to sound propagation with the first few meters of the water column.

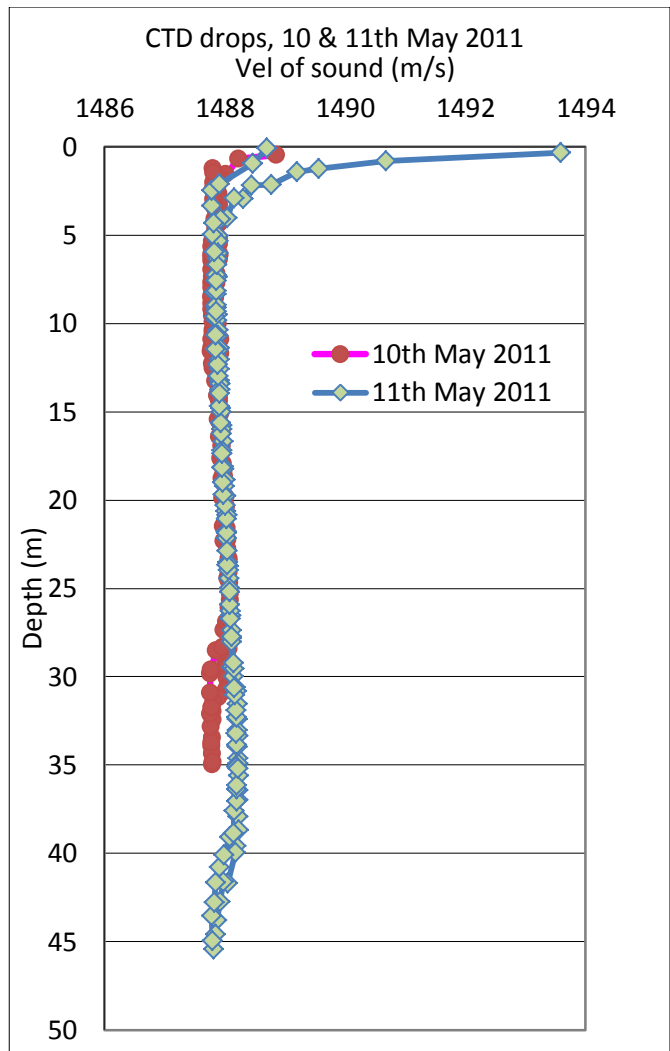


Figure 3-24: CTD profiles 10th and 11th May 2011. Billia Croo.

3.9 WEATHER DATA

Figures 3-25 and 3-26 show significant wave height from wave rider buoys at the EMEC site during the measurement period. Both profiles show relatively low wave heights during the measurement period ranging from 40 – 110 cm, with largest wave height during the initial deployment period.

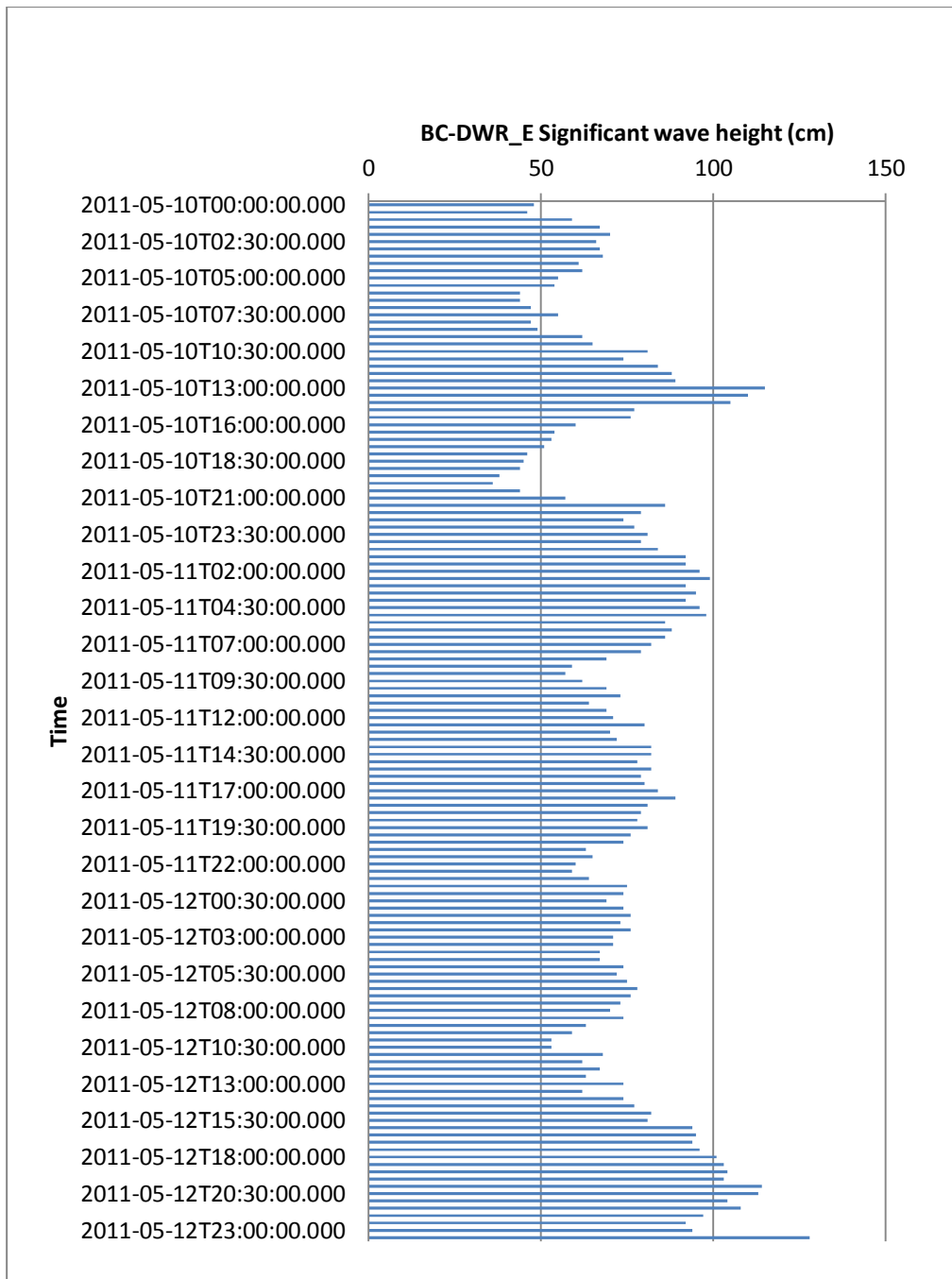


Figure 3-25: Significant wave height 10th-12th May 2011. (wave rider BC-DWR-E)
 [Data provided by EMEC Ltd.]

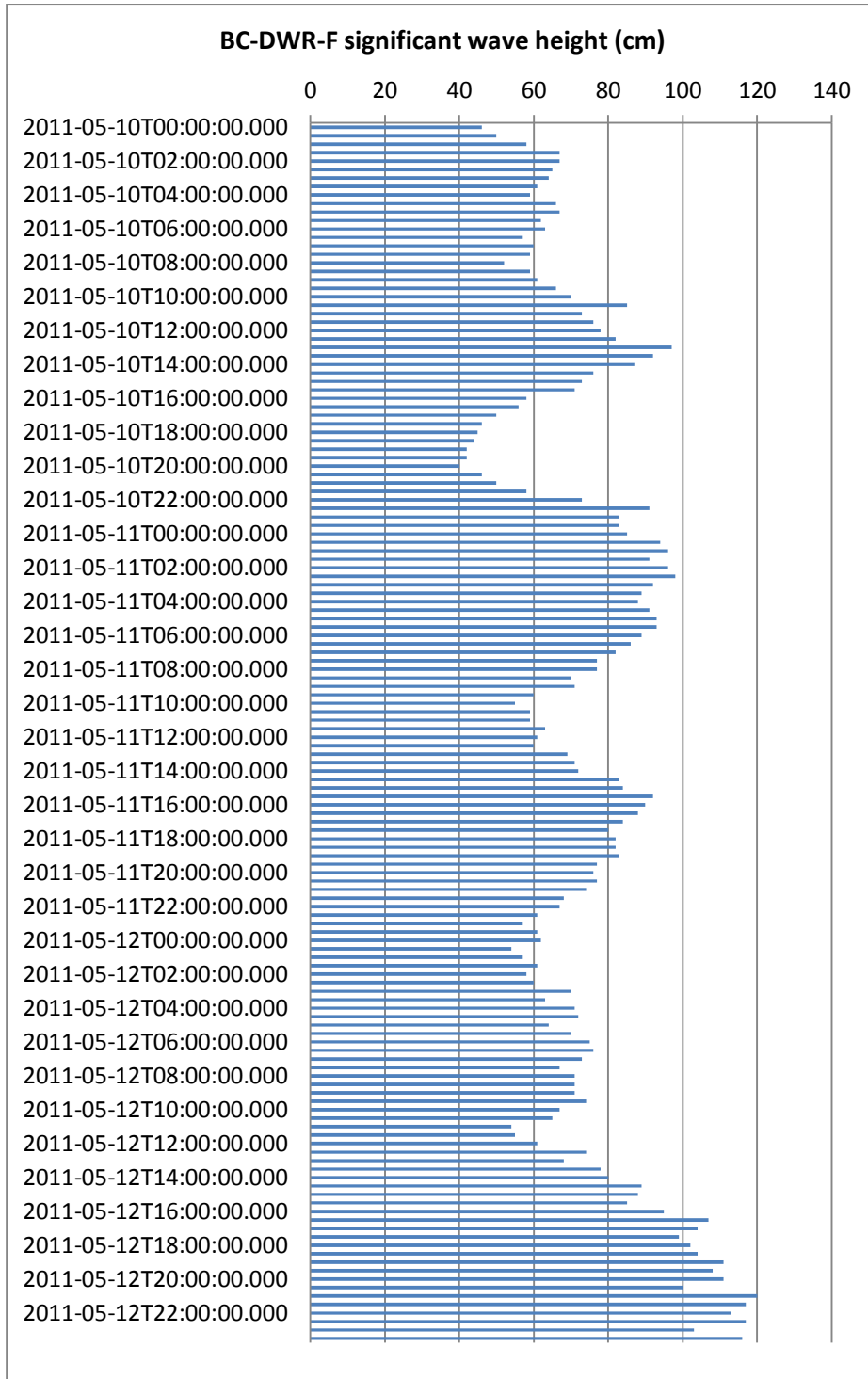


Figure 3-26: Significant wave height 10th-12th May 2011. (wave rider BC-DWR-F)
 [Data provided by EMEC Ltd.]

Analysis of wind speed data (figure 3-27 shows were relatively low (less than 6 ms^{-1}) during most of the trail period. The highest variation seen in the first 12 hours of the deployment with speeds reach 10 ms^{-1} . Windspeeds on the 11th and 12th are consistently below 4 ms^{-1} consistent with good seastates observed during this part of the trial.

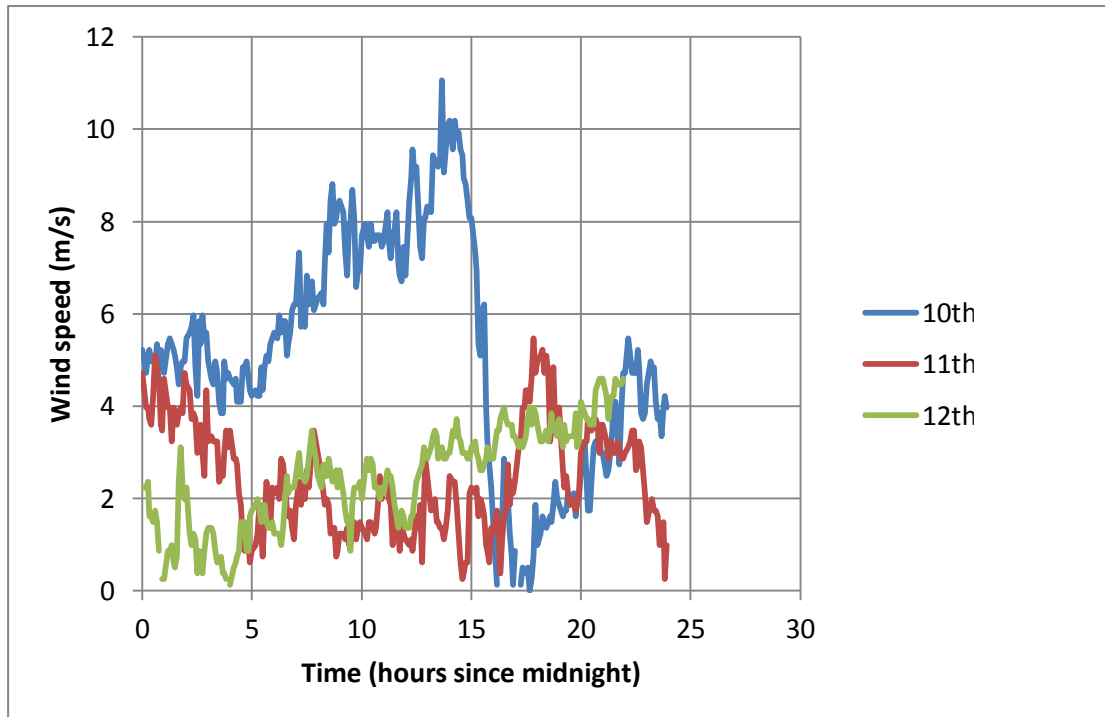


Figure 3-27: Wind speed 10th-12th May 2011.
[Data provided by EMEC Ltd.]

4 SUMMARY

A detailed assessment of the underwater noise output from the Pelamis P2 system was made in May 2011. The purpose of this trial was to validate / develop a measurement methodology for use on wave energy converter systems at the EMEC site. The data obtained during those trials were used to revise the measurement methodology based on lessons learnt. A summary of data obtained and analyses conducted is provided in this report and to the knowledge of authors represents some of the first obtained for this device type.

The measured spectrum of a few tens of Hz to tens of kHz for device noise overlaps with the known hearing response of many marine mammal and fish species [EMEC, 2011a]. The components in range 100 Hz- 2 kHz fall within the known hearing range and above species hearing thresholds of most of the marine mammal species that visit the site [EMEC, 2011b], Southall, 2007]. The audibility or detectability by marine species of device noise is related to relative ratio “critical ratio” of device noise in a specific band to a close by background noise band. Figure 3-18 for example shows higher difference in device and ambient noise levels compared with ambient noise levels without system present at higher sea states increasing likelihood of audibility at greater ranges. By comparison, relative outputs at lower sea-states shown in figure 3-19 would reduce audibility range for components above 300 Hz due to lower relative differences in baseline and device noise. Lower frequency components are, however, still within know frequency range of many fish species and some marine mammals potentially allowing audibility in this case also.

Comparison of device and baseline noise in different sea states shown in figure 3-18 and 3-19 show a significant variation in both baseline and operational noise trials. Comparison of baseline energy in the 100 Hz band shows an increase of around 35 dB with increasing sea states. This variation is higher than traditionally observed for deep ambient water noise curves for a sea state changing over a similar range [Urlick, 1983]. However shallow water ‘ambient’ noise is relatively poorly understood and potential for higher absolute levels and higher variation under different sea state conditions exist. Both cases show elevated noise levels in some bands when closer to the Pelamis system. With a greater difference above equivalent baseline levels at higher sea states.

Source level estimates to device midpoint showed a 10 minute averaged third octave band (CPB) level at around 120 dB re $1\mu\text{Pa}^2\text{Hz}^{-1}\text{-m}^2$ for components in band 10 Hz-2 kHz for sea-state 1-2. At higher sea states (3-4) levels were generally higher with a maximum observed average level in the 1 kHz band of 181 dB re $1\mu\text{Pa}^2\text{Hz}^{-1}\text{-m}^2$. Both frequency of occurrence and the level of some of the potential noise sources from the Pelamis system are likely to be higher at increased sea states as the system becomes more energetic. This may be seen as the increase in the average operational noise levels with increasing sea state. Both data sets suggest not only increased operational noise levels at higher sea state but also increased background levels. The variation between baseline and operational levels is likely to be highly dependent on sea state, local propagation conditions, other noise sources, and devices status etc.

As such outputs from these analyses may be used to further develop understanding of device noise outputs with the aim of improving analysis and measurement exercises, for example future EIA processes. These data, for example, provide a starting point to estimate source terms along lines outlined in the revised methodology [EMEC, 2011c], and in turn allow predictive modelling of device output at a range of different sites. Additional

correlation with device actions may allow attribution of direct acoustic outputs with activity. Data provided in this report has allowed assessment of variation of average short term noise outputs which can be compared for the device under different conditions. In addition, a number of specific acoustic events have been identified.

5 REFERENCES

[Collins, 1993] “A split-step Pade solution for parabolic equation method,” M. D.Collins, J. Acoust. Soc. Am. **93**, 1736-1742, (1993).

[EMEC, 2011a] “Acoustic noise measurement methodology for the Billia Croo European Marine Energy Centre Wave Energy test site (EMEC): Acoustic Baseline measurements”, Paul Lepper, Edward Harland, Stephen Robinson, Peter Theobald & Nichola Quick, Technical report no EMEC_007_09_03, (2011).

[EMEC, 2011b] “Acoustic noise measurement methodology for the Billia Croo European Marine Energy Centre Wave Energy test site (EMEC): Background data review”, Paul Lepper, Edward Harland, Stephen Robinson, Gordon Hastie & Nichola Quick, Technical report no EMEC_007_09_01, (2011).

[EMEC, 2011c] “Acoustic noise measurement methodology for the Billia Croo European Marine Energy Centre Wave Energy test site (EMEC): Measurement methodology for operational noise assessment of WEC systems”, Paul Lepper, Edward Harland, Stephen Robinson, Peter Theobald, Gordon Hastie & Nichola Quick. Technical report no EMEC_007_09_04, (2011).

[Maggi and Duncan, 2010] “Underwater Acoustic Propagation Modelling software –AcTUP V2.2”L, A. L. Maggi and A J. Duncan, Centre for Marine Science and Technology (CMST), Curtin University of Technology in Australia, (2010).

[Southall *et al*, 2007] “Marine mammal noise exposure criteria: Initial scientific recommendations” Southall, B.L., A.E. Bowles, W.T. Ellison, J.J. Finneran, R.L. Gentry, C.R. Greene, Jr., D. Kastak, D.R. Ketten, J.H. Miller, P.E. Nachtigall, W.J. Richardson, J.A. Thomas, and P.L. Tyack. 2007.. *Aquatic Mammals*. 33:1-521, (2007).

[Urlick, 1983] “Principles of underwater Sound”, R.J.Urick, Peninsula Publishing, New York, (1983).

ACKNOWLEDGMENTS

The consortium would like to sincerely thank the teams at Pelamis Wave Power Ltd and E.ON Ltd for assistance during operation trials in 2011 and post analysis phase, all staff at EMEC Ltd particularly David Cowan, Jennifer Norris and Jennifer Falconer and the crew of the Flamborough Light.

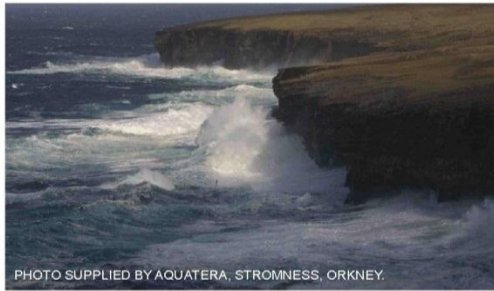
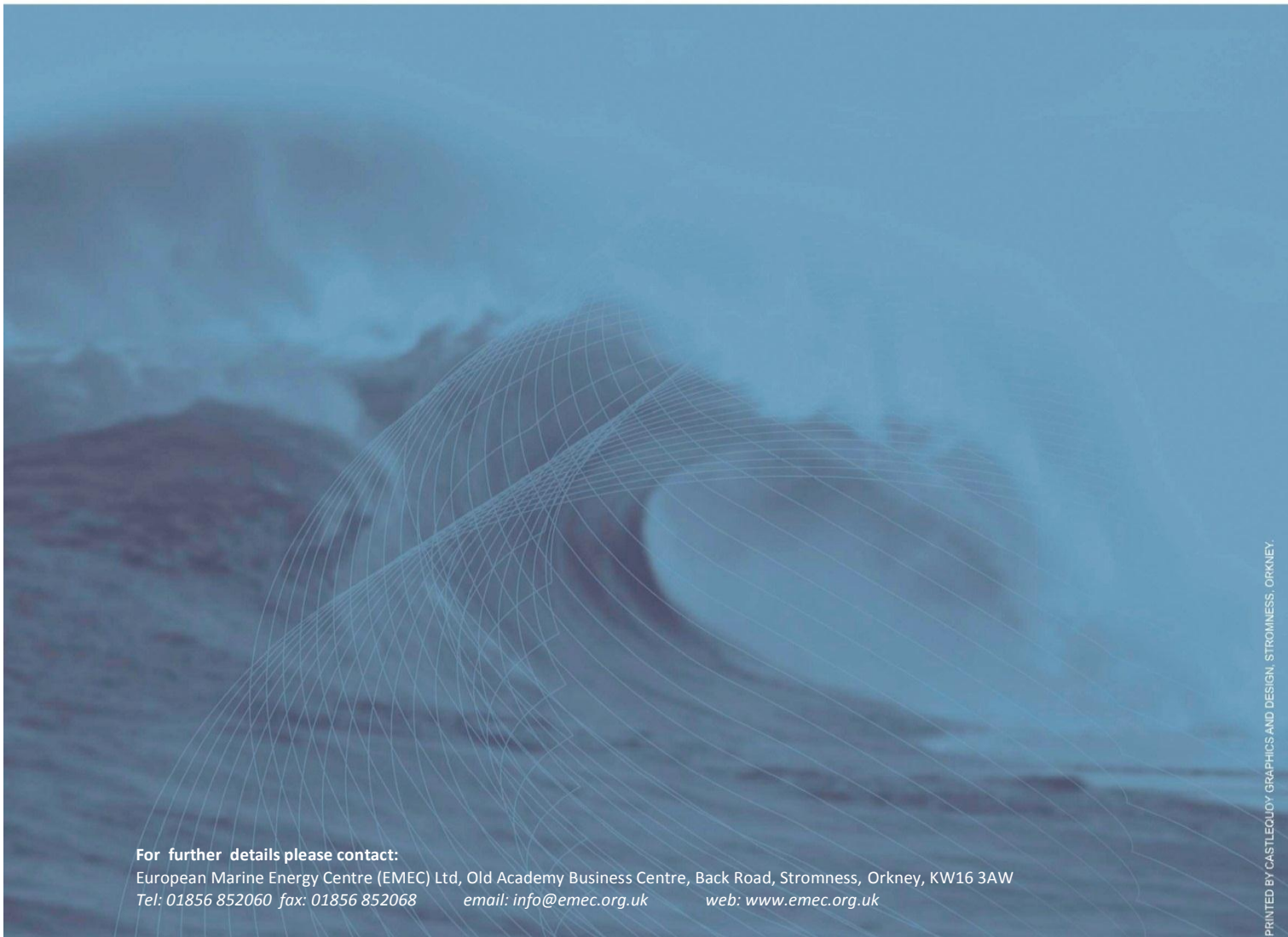


PHOTO SUPPLIED BY AQUATERA, STROMNESS, ORKNEY.



For further details please contact:

European Marine Energy Centre (EMEC) Ltd, Old Academy Business Centre, Back Road, Stromness, Orkney, KW16 3AW
Tel: 01856 852060 fax: 01856 852068 email: info@emec.org.uk web: www.emec.org.uk

PRINTED BY CASTLEQUOY GRAPHICS AND DESIGN, STROMNESS, ORKNEY.

PRODUCED IN ASSOCIATION WITH:



marinescotland



Chickerell
BioAcoustics

